Presented in ECS Spring Meeting Seattle 2018

Fabrication of Lightweight 3D Complex Shapes of Cellular Carbonaceous Materials using Origami

Monsur Islam and Rodrigo Martinez-Duarte

Multiscale Manufacturing Laboratory, Department of Mechanical Engineering, Clemson University, Clemson, South Carolina 29634, USA

We present initial results for the fabrication of lightweight 3D complex shapes of carbonaceous materials using origami technique. 3D complex shapes of carbon materials are fabricated by automated pre-creasing and folding of a flat piece of paper followed by heat treatment in inert atmosphere. The paper origami structure is infiltrated with proper metal precursor before heat treatment in order to fabricate carbide origami shapes. The carbon and carbide origami shape feature low density and exhibits a scaling of elastic modulus with its density, which compares advantageously to other low-density materials. The ongoing work is to improve the mechanical properties of the origami shapes by exploiting the microstructure of the carbonaceous material, optimizing the synthesis process and using different folding geometry of the origami shapes.

Introduction

Cellular carbonaceous materials, particularly carbon and carbide, possess interesting properties including low density, high surface area, high chemical inertness, high oxidation resistance, adjustable electrical conductivity, and high mechanical properties. Due to such properties, they find their use in different applications such as high temperature filters, catalytic support, thermal insulators and structural materials [1,2]. The current state-of-the-art to manufacture cellular carbonaceous materials includes direct foaming method and template method. However, 3D complex shapes, especially with thin cross-sections, are challenging to fabricate in these current techniques.

Here we postulate origami-inspired manufacturing to fabricate 3D complex shapes of carbonaceous material. Origami is an ancient Japanese art of paper folding, where 3D complex shapes of paper can be fabricated by folding of a flat piece of paper along prescribed creases [3–5]. Although historically mostly used as art and for decoration, origami technique has been gaining significant interest due to its potential to fabricate numerous 3D architectures of engineering interest [6]. However, origami folding has so far been limited to the use of paper and soft polymeric sheets. There is no manufacturing technique, that will enable its full potential when employing resilient engineering materials such as metals and ceramics. Sheet metals and composites are relatively thick and stiff and have only been bent into very simple patterns with limited property programming potentials. Hence, there is the need for a manufacturing technique to enable truly versatile origami shaping of engineering materials. Resolving this fundamental

challenge will open up the avenue towards origami-based architectured materials with properties programmed specifically to address performance applications.

Here we present our initial results regarding the fabrication of 3D complex shapes of carbonaceous material. We use a pure cellulose chromatography paper as the carbon precursor. We automate the pre-creasing process and fold the pre-creased paper to obtain 3D origami shape of paper. To obtain carbon structure, we carbonize the paper origami structure. To obtain other carbonaceous material such as carbides, we infiltrate the paper origami structure with a proper metal precursor and heat treat the infiltrated structure at high temperature to facilitate the reaction between the metal and the carbon. We characterize the composition and microstructure of the heat-treated samples. Further, we present the mechanical properties of the carbonaceous origami structures and compare them with other low-density materials.

Materials and Methods

Materials

Our initial target was to fabricate origami structures of glassy carbon and tungsten carbide (WC). Although theoretically numerous shapes can be possible to fabricate, we demonstrated our process using a traditional Miura-ori shape. Here we used Fisherbrand pure cellulose chromatography paper (Sigma Aldrich, Cat. No. 05-714-1) because of its cellulosic nature and minimal impurity. For the synthesis of WC, we used aqueous solution of ammonium metatungstate (AMT, Sigma Aldrich, Cat. No. 463922) as a liquid precursor of tungsten.

Experimental procedure

The fabrication of the carbonaceous material involves three main steps: automatic pre-creasing, manual folding and heat treatment. For synthesis of carbide material, an infiltration step is added before the heat treatment step.

For automatic pre-creasing, we generated CAD models to define the location of the creases. CAD models for the creases on both sides of the paper must be created separately. The chromatography paper was pre-creased using an empty ball-point pen mounted on a cutting plotter machine (Graphtec CE6000-40, USA) using specific equipment parameters. The creasing on the both sides of the paper were automatically aligned by the registration marks generated by the cutting-plotter software and printed on the paper. Figure 1a illustrates an example of a pre-creased paper. Once the pre-creasing was done, the paper was folded manually along the creases to obtain paper origami structures (Figure 1b). The paper origami structure was carbonized at 900 °C for 75 minutes with a heating rate of 5 °C/min in nitrogen environment to obtain origami structures of glassy carbon (Figure 1c). For WC, the paper origami structure was infiltrated with aqueous solution of 20 wt% AMT. The AMT infiltrated origami shapes were heat-treated at 1300 °C for 3 hours with a heating rate of 2.5 °C/min in vacuum environment to obtain WC origami shape (Figure 1d).

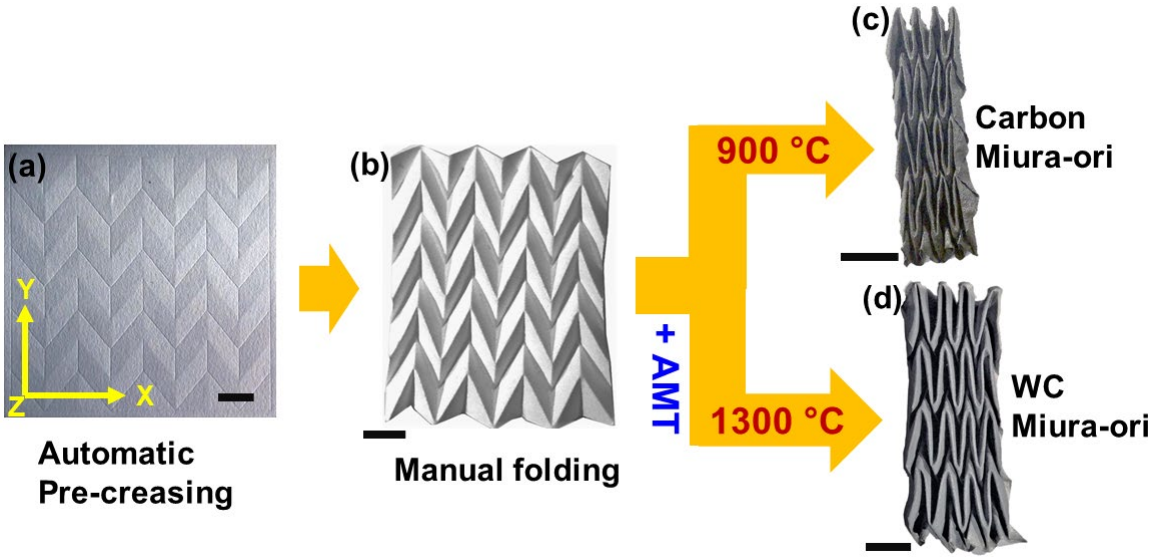

Figure 1: (a) A flat piece of chromatography paper pre-creased using a modified cutting plotter machine. (b) The paper Miura-ori shape obtained by manual folding of the pre-creased paper. (c) Carbon Miura-ori obtained after heat treatment of the paper Miura-ori at 900 °C in nitrogen environment. (d) WC Miura-ori obtained after infiltrating the paper Miura-ori with 20% AMT solution followed by heat treatment at 1300 °C in vacuum environment. The scale bar on each image is 10 mm.

Characterization

The Miura-ori structures obtained after heat treatment were characterized using X-ray diffraction (XRD, Rigaku Ultima IV, Japan) spectroscopy to determine its crystallographic structure and composition of the material. The microstructures of the carbonaceous samples were charecterized using scanning electron microscopy (SEM, S4800, Hitachi, Japan). Following current practices in cellular materials, the structural density (ρ) of the Miura-ori structures was determined by the envelop method, which is the ratio between the mass of the Miura-ori and the total volume it occupied [7,8]. The compression tests of the Miura-ori structures were performed at a rate of 1 mm/min to 80% strain using an Instron Single Column Testing System (Model 5944). A load cell of 50 N was used for the compression tests.

Results and discussion

The XRD pattern of the carbonized paper (Figure 2a) show weak and broad peaks centered around $2\theta = 24°$ and $2\theta = 43°$, which corresponds to (022) and (100) reflections of amorphous carbon [9]. Carbonization of the cellulosic paper results in a porous fibril network of glassy carbon as seen in Figure 2b. The fibers feature an average diameter of 5.26 ± 2.53 µm. The pore size distribution among the fibers are random leading to macroporosity with pore diameter ranging from 1.56 µm to 21.71 µm. The result from the XRD of the heat-treated AMT infiltrated paper (Figure 2c) shows the formation of WC, along with a small amount of W_2C. A significant hump can be seen in the range from $2\theta = 20°$ to $2\theta = 30°$, which suggests a significant amount of carbon of amorphous

nature is present in the material. Our hypothesis is 20% AMT solution does not provide enough tungsten to the carbon matrix. Hence, all the tungsten is carburized into WC and excess carbon remains in the material. The average diameter of fibers forming the fibril matrix of WC is 10.88 ± 2.05 µm (Figure 2d) and the macro-pores caused by the random distribution of the fibers range from 1.04 µm to 28.34 µm.

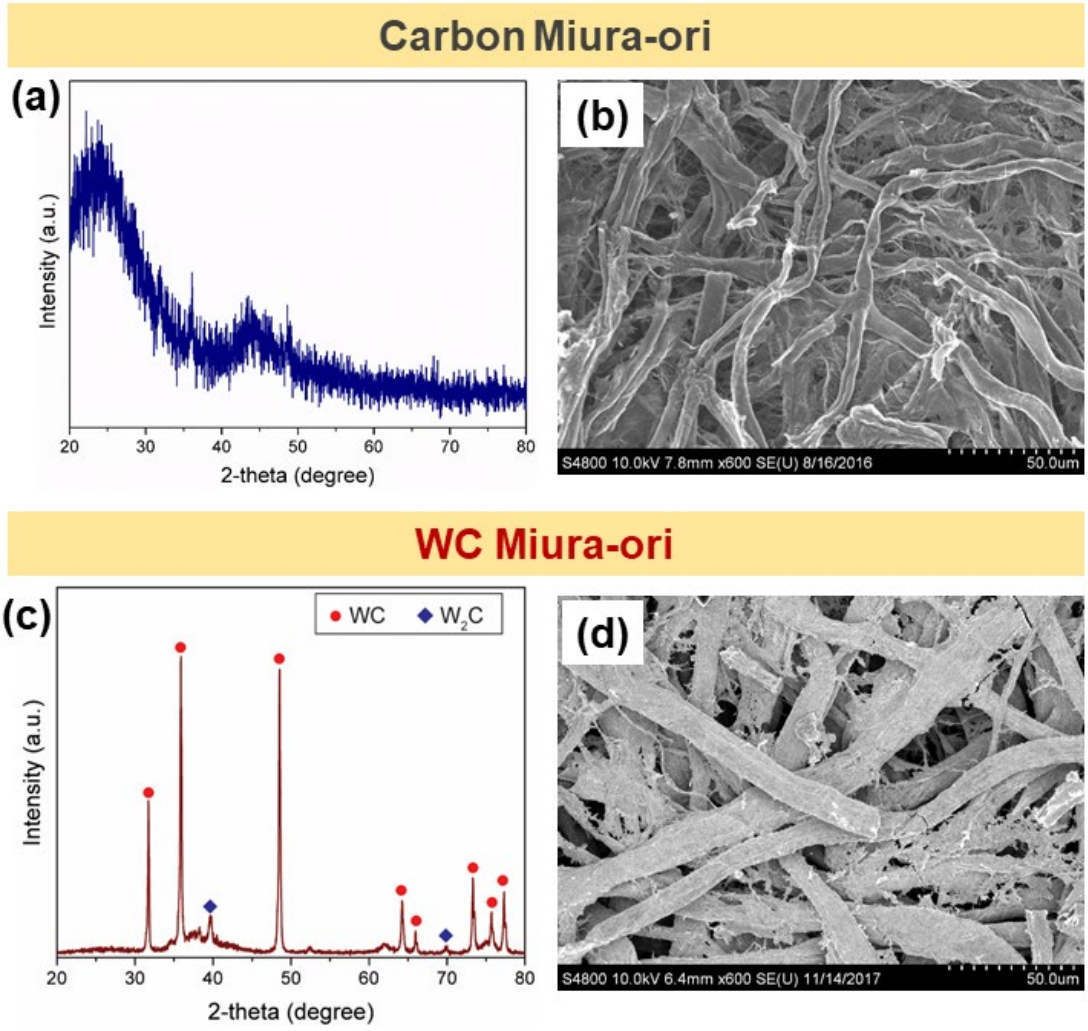

Figure 2: (a) XRD pattern of the carbon origami shapes showing the amorphous nature of the carbon. (b) FESEM image of the carbon origami showing the fibril network of the carbon fibers. The fibers feature an average diameter of 5.26 ± 2.53 µm. (c) XRD pattern of the sample obtained after heat treatment of AMT infiltrated paper origami shape, showing formation of WC in the material. (d) FESEM image of the WC origami showing the fibril network of the WC fibers. The average diameter of fibers is 10.88 ± 2.05 µm.

A significant shrinkage occurred in the overall structure of the Miura-ori for both carbon and WC material during the heat treatment process as shown in Figure 1. The amount of shrinkage in different direction (See Figure 1) is listed in the Table I. In both the cases, the maximum amount of shrinkage occurred in the X-direction. However, the shrinkage in Y- and Z-direction is almost similar. Along with the material release during the heat treatment, the mechanics of the Miura-ori structure plays a strong role in the shrinkage. The Miura-ori structure experiences compressive stresses due to the thermal

contraction resulted in during the cooling step [10]. The Miura-ori structure is more susceptible to compression in X-direction than the other two directions. Hence, maximum amount of shrinkage occurred in the X-direction during the thermal contraction.

TABLE I. Structural shrinkage of carbon and WC Miura-ori.

Direction	Shrinkage (%)	
	Carbon Miura-ori	**WC Miura-ori**
Along X	73.51 ± 4.69	51.22 ± 4.9
Along Y	33.94 ± 2.89	21.61 ± 0.98
Along Z	38.48 ± 1.74	20.09 ± 3.28

The stress-strain curve obtained in the compression test had three distinct regions: the elastic region, post-yielding softening and densification [11,12]. We calculated the elastic modulus (E) as the slope of the elastic region of the stress-strain curve. This elastic region is characterized by the fact that the panels can stretch away from the creases to absorb the compression force. The elastic moduli for the carbon and WC Miura-ori structures are plotted in Figure 3 against their corresponding density. The E for carbon Miura-ori ranges from 0.0165 MPa to 0.246 MPa for a density range of 0.088 g/cm^3 to 0.035 g/cm^3. On contrary, the WC Miura-ori featured an E ranging from 0.052 MPa to 0.293 MPa for a density range of 0.04 g/cm^3 to 0.126 g/cm^3. The density of the WC structures were heavier than the carbon Miura-ori shapes. This was expected as WC is a heavier material compared to carbon material. However, we expected to obtain significant improvement in the elastic modulus in the case of WC Miura-ori, which did not happen. Our hypothesis is the excess carbon present in the WC Miura-ori results in such elastic modulus for the WC Miura-ori samples. The ongoing work is to optimize the synthesis process to obtain only WC. We expect to achieve higher mechanical properties for the origami structures with only WC.

The elastic modulus of a cellular material relates to its density, which follows Ashby-Gibson's scaling law (Equation 1).

$$E \alpha \rho^{n} \quad [1]$$

n is the scaling exponents which represents the failure mode of the material such as bending or stretching. The value of n depends on the microstructure of the material, material composition and geometry of the cellular material which includes cell type (open or closed), geometrical arrangement of the cells and size of the cells [13]. For a stretch dominant material the value of n is 1, whereas the value of n for a bending dominant material is 2 [14]. As seen from Figure 3, the carbon and WC Miura-ori structures feature an n of 1.76 and 1.79 respectively. Hence, although the material composition and the microstructural properties are different both the cases, the scaling exponent is very similar for both the cases. Our hypothesis is the geometrical structures of the origami is the dominant factor over the microstructure and the material composition while determining the scaling exponent. The scaling exponent of the Miura-ori structures of

both the materials suggests they feature a bending dominant failure mode under compressive load similar to other open cell cellular material. This is expected as the Miura-ori structure does not contain any lateral member or panel to carry tensile load, which is an important feature for a stretch dominant material [15].

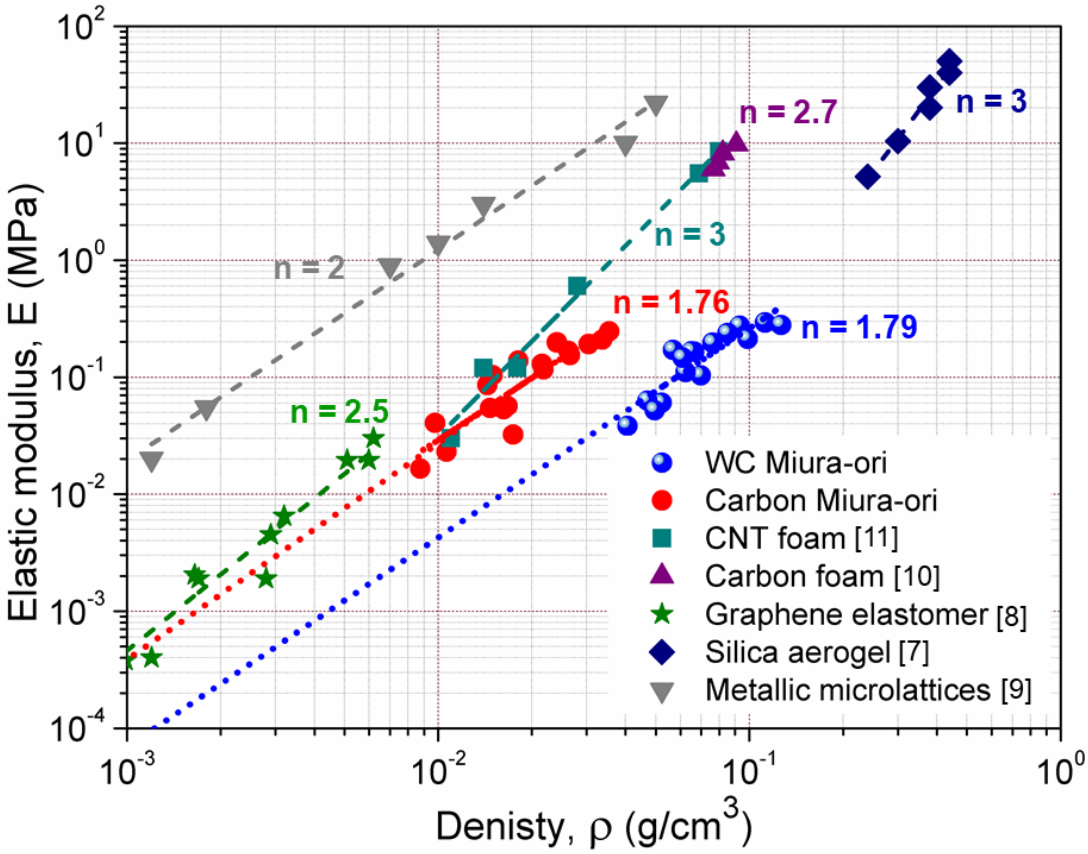

Figure 3: The elastic modulus of the carbon and the WC Miura-ori shapes against their densities. The carbon origami features a scaling of $E \sim \rho^{1.76}$, whereas the WC origami exhibits a scaling of $E \sim \rho^{1.79}$. Elastic modulus of other low-density materials is also plotted here to compare our origami structures with other low-density materials.

We further compared the elastic modulus of the carbon and WC Miura-ori with other popular lightweight cellular material. The scaling of the carbon and WC Miura-ori compares advantageously with these low-density cellular materials. For example, silica aerogel and carbon nanotube (CNT) foams feature a $n = 3$ [7,16]; carbon aerogels feature a $n = 2.7$ [17]; Metallic microlattices feature a $n = 2.4$ [18]; and graphene elastomer features a $n = 2.5$ [19]. This suggests the Miura-ori has better load carrying capabilities while compared to these low-density materials. However, the elastic moduli of the Miura-ori structures are lower at a given density while comparing to the elastic modulus of most of these low-density materials. Obtainment of homogenous WC is expected to improve the elastic modulus of the WC Miura-ori. Further, the mechanical properties of the Miura-ori structures are expected to improve by using paper featuring smaller fiber diameter and lower pore size distribution [20]. Our ongoing work is on characterization of the mechanical properties of the carbon and WC origami structures using papers

having different microstructures to understand the impact of the microstructure and improve the mechanical properties.

Conclusion

Here, we demonstrated the origami technique to fabricate of lightweight 3D complex shapes of carbon and WC material. We pre-creased a flat piece of paper using a cutting-plotter machine to facilitate manual folding of paper origami shapes. The paper origami shapes were carbonized to obtain the carbon origami shapes. To fabricate WC origami shapes, we infiltrated the paper origami shapes with AMT and heat treated them in vacuum atmosphere. Both the carbon and WC origami structure feature fibril microstructure. The origami shapes feature low density comparable to other low-density materials, such as CNT foam and metallic microlattices. These origami shapes exhibit better scaling of the elastic modulus while compared to other low-density material. However, the elastic modulus is not superior to that of the other low-density materials.

Our ongoing work is to improve the mechanical properties of the origami structures by exploiting the microstructural properties of the carbonaceous materials, optimizing the synthesis protocol and using different folding geometries of the origami shapes.

Acknowledgments

Monsur Islam acknowledges support from Hitachi through a High Technologies Fellowship. The authors are thankful to the Institute for Biological Interfaces of Engineering for facilitating the mechanical testing.

References

1. M. Inagaki, J. Qiu, and Q. Guo, Carbon N. Y. **87**, 128 (2015).

2. L. Borchardt, C. Hoffmann, M. Oschatz, L. Mammitzsch, U. Petasch, M. Herrmann, and S. Kaskel, Chem. Soc. Rev. **41**, 5053 (2012).

3. L. H. Dudte, E. Vouga, T. Tachi, and L. Mahadevan, Nat. Mater. **15**, 583 (2016).

4. D. Dureisseix, Int. J. Sp. Struct. **27**, 1 (2012).

5. A. Lebée, Int. J. Sp. Struct. **30**, 55 (2015).

6. M. Schenk and S. D. Guest, in *Origami 5 Fifth Int. Meet. Origami Sci. Math.* (CRC Press, Boca Raton, FL., 2011), pp. 291–304.

7. M. A. Worsley, S. O. Kucheyev, J. H. Satcher, A. V. Hamza, and T. F. Baumann, Appl. Phys. Lett. **94**, 1 (2009).

8. S. M. Manocha, K. Patel, and L. M. Manocha, Indian J. Eng. Mater. Sci. **17**, 338 (2010).

9. V. Palmre, E. Lust, A. Jänes, M. Koel, A.-L. Peikolainen, J. Torop, U. Johanson, and A. Aabloo, J. Mater. Chem. **21**, 2577 (2011).

10. W. S. Kwon and K. W. Paik, Int. J. Adhes. Adhes. **24**, 135 (2004).

11. S. Callcut and J. C. Knowles, J. Mater. Sci. Mater. Med. **13**, 485 (2002).

12. A. Celzard, W. Zhao, A. Pizzi, and V. Fierro, Mater. Sci. Eng. A **527**, 4438 (2010).

13. O. M. Istrate and B. Chen, Soft Matter **7**, 1840 (2011).

14. M. F. Ashby, Philos. Trans. A. Math. Phys. Eng. Sci. **364**, 15 (2006).

15. X. Zheng, H. Lee, T. H. Weisgraber, M. Shusteff, J. DeOtte, E. B. Duoss, J. D. Kuntz, M. M. Biener, Q. Ge, J. a Jackson, S. O. Kucheyev, N. X. Fang, and C. M. Spadaccini, Science **344**, 1373 (2014).

16. N. Leventis, C. Sotiriou-Leventis, G. Zhang, and A. M. M. Rawashdeh, Nano Lett. **2**, 957 (2002).

17. R. W. Pekala, C. T. Alviso, and J. D. LeMay, J. Non. Cryst. Solids **125**, 67 (1990).

18. T. a. Schaedler, a. J. Jacobsen, a. Torrents, a. E. Sorensen, J. Lian, J. R. Greer, L. Valdevit, and W. B. Carter, Science (80-.). **334**, 962 (2011).

19. Z. Qin, G. S. Jung, M. J. Kang, and M. J. Buehler, Sci. Adv. **3**, 1 (2017).

20. I. Keun Kwon, S. Kidoaki, and T. Matsuda, Biomaterials **26**, 3929 (2005).